

An overview of bio-interface electrolyte and $\text{Li}_2\text{FePO}_4\text{F}$ as cathode in Li-ion batteries

Thu Thi Pham¹, Majid Monajjemi^{1,2,*}, Dung My Thi Dang¹, Fatemeh Mollaamin¹, Aboolfazal Khakpour³, Chien Mau Dang¹

¹Institute for Nanotechnology (INT), Vietnam National University - Ho Chi Minh City (VNUHCM), Ho Chi Minh City, Vietnam

²Department of chemical engineering, Central Tehran Branch, Islamic Azad University, Tehran, Iran

³Department of chemistry, Ayatollah Amoli Branch, Islamic Azad University, Amol, Iran

*corresponding author e-mail address: Maj.monajjemi@iauctb.ac.ir

ABSTRACT

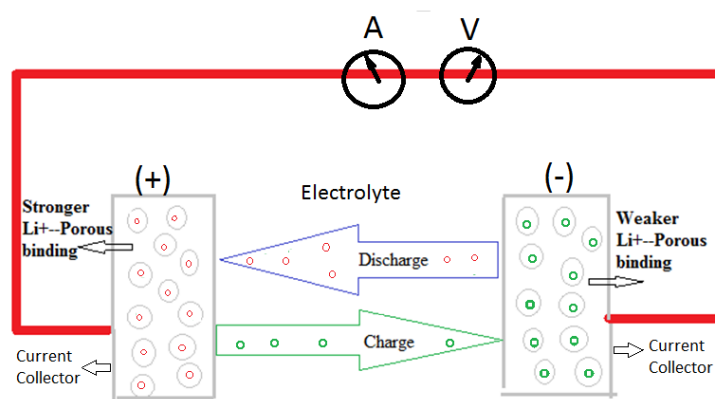
Composites of $\{[(1-x-y) \text{LiFe}_{0.333}\text{Ni}_{0.333}\text{Co}_{0.333}] \text{PO}_4\}$, $x\text{Li}_2\text{FePO}_4\text{F}$ and $y\text{LiCoPO}_4$ system were synthesized using the sol-gel method. Stoichiometric weights of the mole-fraction of LiOH , $\text{FeCl}_2 \cdot 4\text{H}_2\text{O}$ and H_3PO_4 , LiCl , $\text{Ni}(\text{NO}_3)_2 \cdot 6\text{H}_2\text{O}$, $\text{Co}(\text{Ac})_2 \cdot 4\text{H}_2\text{O}$, as starting materials of lithium, Iron, Nickel, and Cobalt, in 7 samples of the system, respectively. We exhibited $\text{Li}_{1.167}\text{Ni}_{0.222}\text{Co}_{0.389}\text{Fe}_{0.388}\text{PO}_4$ is the best composition for cathode material in this study. Obviously, the used weight of cobalt in these samples is lower compared with LiCoO_2 that is an advantage in view point of cost in this study. Charge-discharge characteristics of the mentioned cathode materials were investigated by performing cycle tests in the range of 2.4–3.8 V (versus Li/Li^+). Our results confirmed, although these kind systems can help for removing the disadvantage of cobalt which mainly is its cost and toxic, the performance of these kind systems are similar to the commercial cathode materials in Lithium Ion batteries (LIBs).

Keywords: lithium ion battery, LiCoPO_4 , $\text{Li}_2\text{FePO}_4\text{F}$, sol-gel method, cathode materials.

1. INTRODUCTION

Among the all batteries, some of them, such as NiMH (nickel metal hydride) and lithium ion batteries (LIBs) have the most efficiency for electric vehicles (EVs), hybrid electric vehicles (HEVs) and so on. Although the vehicle bazaar is dominated by NiMH market, the LIBs have received centralized research and progress due to its high energy density, cathode materials diversity, long and stable cycle life, suitable initial charge and discharge, high voltage and excellent environmental friendly [1-3]. Structure of various Li-ion batteries basically requires the optimum estimation for conductivities and diffusivities, in order to both predicting and designing of several improved materials. So far, lithium ion batteries have been mostly applied in a wide range of portable, cell phones, cameras and many other smart devices [4, 5]. For HEVs and EVs systems, however, the efficiency of LIBs, especially their energy densities, cost, voltage and safety must be improved yet. LIBs are combined of three major sections including, anodic Li^+ intercalation, cathode, and the electrolyte-separator. During charging, lithium cations via the electrolyte-separator section move from the cathode to the anode side and back when discharging, meanwhile the electrons flow out of the external circuit for providing the electrical power (Scheme 1). Although the performance of LIBs depends on several items, basically the efficiency strongly relies on the composition of the electrolyte substance and property of the cathode material structures [6-8]. As instance for LiMO_2 ($\text{M}=\text{Co}, \text{Mn}, \text{Ni}, \dots$) as cathode materials there is two directions, in first item during charging, lithium ions move from positive side to negative electrode and electrons are removed from cathode by an external field and then are transferred to anode. In the second item, during discharge, anode provides the ions to electrolyte and electrons to the external circuit where the ions intercalate into cathode materials and electrons from the external circuit for charge

restoration as following reactions. In Positive electrodes $\text{LiMO}_2 \rightleftharpoons \text{Li}_{1-x}\text{MO}_2 + x \text{Li}^+ + x \text{e}^-$ and the negative electrode reaction as: $x\text{C}_6 + x \text{Li}^+ + x \text{e}^- \rightleftharpoons x\text{LiC}_6$ with the whole reaction as: $\text{LiMO}_2 + x\text{C}_6 \rightleftharpoons \text{Li}_{1-x}\text{MO}_2 + x\text{LiC}_6$.



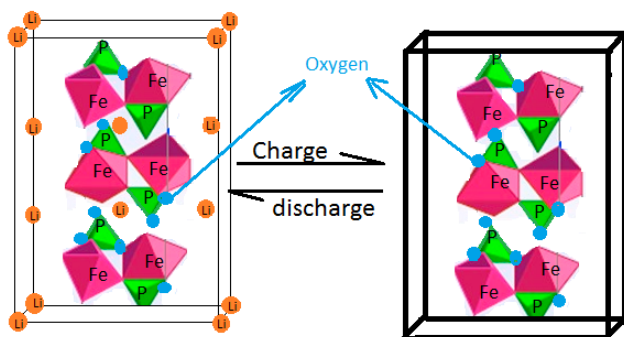
Scheme 1. The spheres are the active particles of the two porous electrodes in which Li^+ ions; can be stored. The voids between particles and between the electrodes are filled with an electrolyte in which Li^+ diffuse and migrate thermodynamically.

Initially, in 1991 the Sony Corporation focused on LiCoO_2 materials as an important layered structure [9-12]. Then the other layered structure such as LiNiO_2 has been applied [13-15]. This layered cathode material displayed favorable specific capacities, but safety reasons and structural instability prevented further development. The other layered structures such as LiMnO_2 and LiFeO_2 were selected due to redox couples advantages of $\text{Fe}^{4+}/\text{Fe}^{3+}$ and $\text{Mn}^{4+}/\text{Mn}^{3+}$. Unfortunately the preparing of electrochemically active LiFeO_2 phases was not possible and for LiMnO_2 , though easy to prepare had problem about the structural instability due to the layered phase reversing to spinel LiMn_2O_4 during cycling [16,17].

1.1 Cathode material.

Many commercial batteries have been made of cathode materials with two kind classification first, some cathode material such as LiTiS_2 consist of anions close-packed which the alternate layers are localized between the anion plates and are occupied with the redox-active transition metals, while Li inserts into the empty remaining layers., followed. Second, a Large series of (+) materials have been investigated and are applied commercially in LIBs as cathode materials which can generally be categorized based on structure types such as olivine structure (LiFePO_4), layered structure (LiCoO_2 , LiNiO_2 , Li_2MnO_3 , $\text{LiNi}_{1-x}\text{Co}_x\text{O}_2$, $\text{LiNi}_{1/3}\text{Mn}_{1/3}\text{Co}_{1/3}\text{O}_2$) and spinel structure (LiMn_2O_4) which have a three dimensional framework shape.

1.1.1 Olivine structure. LiFePO_4 [18] can be applied at 95% of its theoretical capacities and 160mAh/g with suitable rate capabilities which is currently being selected as a candidate cathode material for next generation Li-ion batteries [19]. LiFePO_4 has an olivine structure (scheme.2) which is very different from the layered and spinel structures of other lithium-ion chemistries. The intercalation mechanism is also different, involving phase changes. LiFePO_4 has a specific capacity about 160mAhg⁻¹ and an average voltage around 3.40V [18-21]. LiFePO_4 has more advantage due to inexpensive and environmentally friendly. In recent decades there have been centralized researches in improving the performance of Li-ion batteries in viewpoints of cathode materials. The cathode materials in the second group of Mendeleev's table have large tunnel structures, such as vanadium oxides, manganese dioxide, and transition-metal phosphates which potentially has lower cost (olivine LiFePO_4) [22].

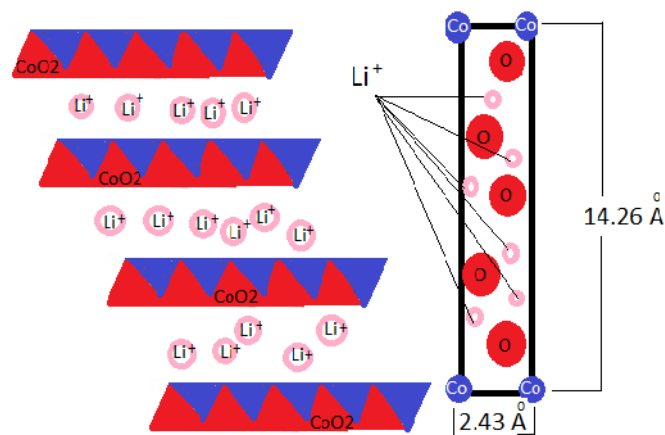


Scheme 2. LiFePO_4 during charge and discharge.

The tunnel structure of LiFePO_4 (where errant Fe ions in the Li sites) can reduce reactivity and diffusion of lithium. For LiFePO_4 , the discharge potential is about 3.5 V vs. lithium and no explicit capacities fading were appeared even after a couple hundred cycles and its capacity (175 Ahkg⁻¹) is higher than commercial LiCoO_2 with high stabilizing even more than LiNiO_2 [23]. LiFePO_4 can be synthesized through hydrothermal conditions, or by sol-gel experiments [23].

The structure LiFePO_4 is consist of about 6.5% iron atoms in the lithium site with lattice parameters of a : 10.38 Å, b : 6.011 Å, and c : 4.71 Å compared with those for ordered LiFePO_4 of a : 10.33 Å, b : 6.012 Å, and c : 4.69 Å. Therefore the Fe atoms basically block diffusion of the Li^+ , while diffusion effect along the tunnel is faster [23, 24] (scheme 2).

1.1.2 Layered structure. This structure generally has layered similar $\alpha\text{-NaFeO}_2$ shape, that is a distorted rock-salt while the cations replaced in alternating (1 1 1) planes. In this structure the oxygen is placed in a centered cubic close-packed arrangement with the metal oxide, and the lithium ions would reside in the spaces among the oxygen layers. These kind structures help the intercalation process that the lithium cations are alternately diffused and removed from the structures during charge and discharge cycles [25]. The LIBs commercially is overmatched by an important layered structure as known “ LiCoO_2 “, which firstly prepared by Sony’s company in 1991. LiCoO_2 has $\alpha\text{-NaFeO}_2$ position with oxygen atoms which are replaced in a cubic arrangement, as soon as Li atoms are completely removed; the oxygen layers rearranged themselves for giving hexagonal close packing in form of CoO_2 (Scheme.3). This cathode material exhibits an initial discharge capacity around “145mAhg⁻¹” with an expectation voltage of “3.75 V”. Also improvements were demonstrated in the cycle-ability for this material when doped with transition metal such as Mg or Al. As LiCoO_2 is suitable material for commercial batteries several compositions are being studied via a solid solution with LiCoO_2 including, “ $\text{Li}_2\text{MnO}_3\text{-LiCoO}_2\text{-LiNiO}_2$ ” [26], $\text{LiCoO}_2\text{-Li}_2\text{MnO}_3$ [27], $\text{LiNi}_{1/2}\text{Mn}_{1/2}\text{O}_2\text{-Li}_2\text{MnO}_3\text{-LiCoO}_2$ [28, 29] and $\text{LiNiO}_2\text{-LiCoO}_2$ [30].



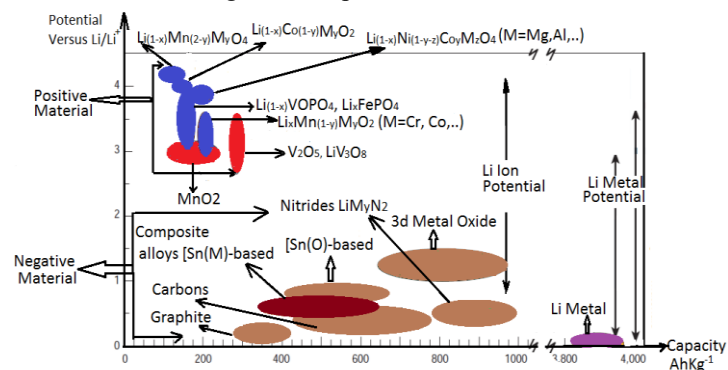
Scheme 3. Models of the layered LiCoO_2 .

1.1.3 Spinel structure. The spinel cathode material such as LiMn_2O_4 has discussed by Thackeray et al and has been widely investigated by the Bellcor labs, and Amatucci [31]. The anion contains cubic close-packed oxygen and although is similar to the R-NaFeO_2 layer structure, there is a difference only in the distribution of the cation among the free sites of octahedral and tetrahedral position. The spinels might be imaged as a special form where the transition-metal cation is placed in all the layers therefore there are more open structures (like vanadium oxides) and also tunnel compounds of manganese dioxide or the transition-metal phosphates, such as the olivine LiFePO_4 . The various potential cathode materials versus Li/Li^+ related to their applied capacities are presented in the scheme 4.

1.2. Solvent-Interface Materials & Electrolytes.

LIBs contain an anode, a cathode, and an electrolyte. The electrolyte is necessary for separating two major components of ionic and electronic transporting. In an ideal battery the Li^+ transport number will be unit in the electrolyte and the potential

can be estimated through the difference between the standard chemical As mentioned, the Li^+ flow via the electrolyte and separators, while the electrons move through the external circuit in system. Obviously, both of electrodes should allow for flow the Li^+ through suitable ionic and electron conductors. Potentials of the lithium in the negative and positive electrodes $\Delta G = n E F$.



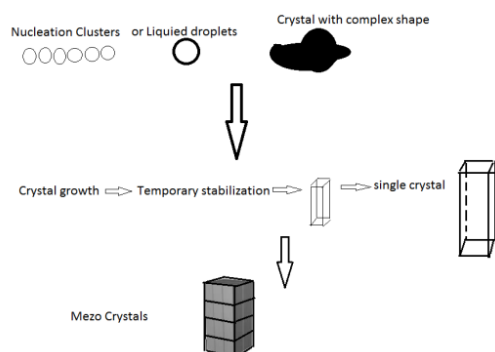
Scheme 4. Various potential cathode materials versus Li/Li^+ .

It is important to consider many electro-chemical activated materials are not suitable electronic conductors, so it is needed for adding the sensitive electronic conductive material such as carbon. For any mechanical holding of the electrodes together, a strong binder is also needed. The electrolyte solutions generally comprise Li salt dissolved in a liquid of organic solvent such as LiPF_6 or Li-BOB (BOB is an anion including two boron which is coordinated with two oxalate groups) in an ethylene carbonate/dimethyl carbonate solvent. Although Biopolymers including Li^+ have been applied in recent years as electrolytes, their conductivities are still so much important item for any investigation of the efficiency in

2. MATERIALS AND METHODS

2.1. Synthesis of LiFePO_4 .

Meso-crystal structures [34-37] have 3D- superstructures which their morphologies are composed of a few to hundreds of nano-scaled primary units (around 1-900 nm) [34]. Meso-crystal has been initially demonstrated in bio-minerals. The formation of meso-crystals has been accomplished via a processing such as parallel crystallization, colloidal assemblies and controlled structure formation from nanoparticle building units [38] (scheme.5).



Scheme 5. Presentations of different crystallization pathways leading to the formation of meso crystals.

The morphology of the LiFePO_4 is of primary importance for the electrochemical properties, as the rate performance, conductivities and capacities of the of lithium-ion battery cells. The application

LIBs. Therefore they are only applied during the related liquids are added for giving a plasticized state. In addition, some solid electrolyte has been considered for several specialized electrolytes. Although the Li^+ flow inside the various electrolytes, the two electrodes should be separated for preventing an electrical short. It is done with using various porous separator materials. An important research [32], confirmed the excellent results of surfaces coating. This mechanism is depended on minimization in the reactivates of Co^{4+} with HF in electrolytes which is related to the interaction of moisture with those electrolyte's salts such as LiPF_6 .

1.2.1. Molten Salt Systems. Occasionally, LIBs batteries used the molten salts as electrolyte which acted at around 500°C . Although the first cells applied both molten lithium and sulfur as two electrodes, the problems with interface of electrolyte – electrodes reaction appeared in the cell. Although it is a goal for developing a cell based on the lithium/sulfur, a system at low temperatures around -35°C in electrolyte solvents of di-oxolane and dimethoxy-ethane has been investigated [33]. This cell with its liquid poly-sulfides cathodes has produced specific power 745 W/kg at 24°C . Recently, the lithium anode from the reactive poly-sulfides is to coat it with the single-ion conducting glasses. One of the most important electrolytic behaviors is $\text{Na}_{1+x}\text{Al}_{11}\text{O}_{17}$, which has been used as the electrolyte for a battery including molten sodium as anode and molten sulfur as cathode at 310°C which mixed vanadium oxide ($\text{Li-Li}_x\text{V}_2\text{O}_5$) also applied as electrodes for both NIBs and LIBs[33].

of LiFePO_4 Meso-crystalline needs the poly (vinyl pyro-lidone) or other surfactants as growth-directing agents during the synthesis.

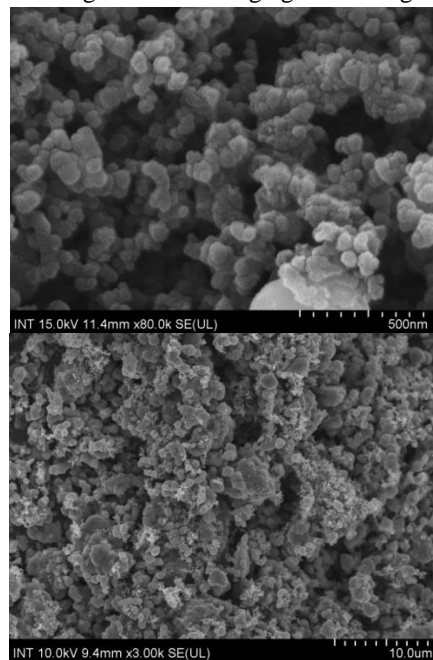


Figure 1. SEM of LiFePO_4 .

The cells were charged and discharged at room temperature in the voltage range of $2.4\text{--}3.8\text{ V}$ (versus Li/Li^+).



Scheme 6. The glove Box model kk-011AD in institute for nanotechnology, Vietnam National University-Ho Chi Minh City

LiFePO_4 Meso-crystals can be synthesized through low-temperature solvent-thermal reaction as follows. The initial solutions were prepared via dissolving stoichiometric mole-fraction of LiOH , $\text{FeCl}_2 \cdot 4\text{H}_2\text{O}$ and H_3PO_4 in 25 milliliter ethanol under strong mechanical stirring for an hour. The prepared, clear green solution has been covered in a glass of a Teflon autoclave

3. RESULTS

The purpose of this study is to find a ternary solid solution of Li-based cathode material that is an advantageous replacement for LiCoPO_4 which is expensive and toxic (based on our previous works)[40-68]. Therefore a combination of ternary composition diagram including $\{(1-x-y) \text{LiFe}_{0.333}\text{Ni}_{0.333} \text{Co}_{0.333}\} \text{PO}_4$, $x\text{Li}_2\text{FePO}_4\text{F}$ and $y\text{LiCoPO}_4$ composite have been considered. In viewpoint of electrochemical behavior which indicates manganese is +4, which remain without Jahn-Teller distortion with the +3 valance (Mn^{+3}). Solid solutions were basically elected in terms of obtaining a cathode composition with superior efficiency of cycle-ability, capacity and structural stabilities also with costs low. By a few works the solid solutions have been applied as cathode material including both binary and ternary systems. It is notable that the initial crystal structures of the cathode material not only specifies the initial characteristic capacity, but also imply to the stability. The consistency of de-lithiated cathode materials is substantial for any increase of the cycle life. So through substituting some atoms of Mn with Fe atoms the total metal-oxygen bonding of the material is going to be stronger than the cathodes because the 3d state of Mn^{4+} is $3d^3 (t_{2g}^3 e_{2g}^0)$.

This investigation is used for finding the best cathode material compositions of $\{(1-x-y) \text{LiFe}_{0.333}\text{Mn}_{0.333} \text{Co}_{0.333}\} \text{PO}_4$, $x\text{Li}_2\text{FePO}_4\text{F}$ and $y\text{LiCoPO}_4$ with high initial discharge capacity, grate cycle-ability and inexpensive cost compared to current lithium-ion cathode materials. Therefore, initially, 28 different composition points according to using the lever rule, stoichiometric weights and mole-fractions were chosen in order to find an optimized material with good electrochemical performance. These 28 points were extracted through the triangle phase diagram of the defined system [Fig.2 and table 1&2] and synthesis through sol-gel method.

which was then heated up in an oven to 250°C and high pressure for overnight. LiFePO_4 Meso-crystals took place inside the autoclave during solvent-thermal processing, and also the reactor was allowed for cooling down up to 25°C with water bath. The collected green precipitate has been washed completely with water and was dried under vacuum at 70°C . Carbon coating on the surface of LiFePO_4 Meso-crystals, N-acetyl-lglucos-amine ($\text{C}_5\text{H}_{15}\text{NO}_6$, 0.2 g) was added in the precursor solution before the autoclave treatment. For increasing the crystal stabilities of material and also the conductivities of the carbon layers, Glove-Box model of kk-011AD (serial No: kk-1760) have been used at it is atmosphere (scheme.6). The final pristine LiFePO_4 powder was very pure and green and also the final LiFePO_4 carbon/meso-crystal composites were black in color in Fig.1 the SEM of LiFePO_4 are shown.

The composites were synthesized using the sol-gel method due to simple chemical reaction with a low temperature and a high degree of homogeneity. For fabrication of cathodes, the prepared products were first mixed with acetylene black and poly-vinylidene fluoride in N-methyl-pyrrolidone (NMP).

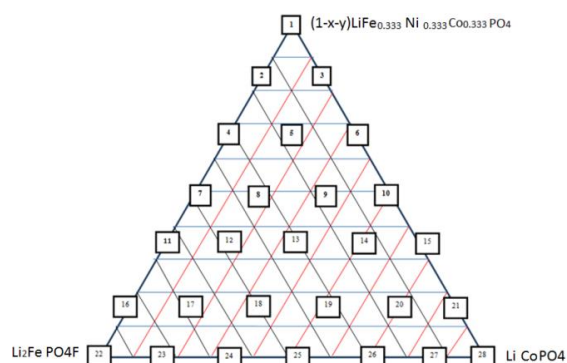


Figure 2. Binary and Ternary diagram of $[(1-x-y) \text{LiFe}_{0.333}\text{Ni}_{0.333}\text{Co}_{0.333}] \text{PO}_4$, $x \text{Li}_2\text{FePO}_4\text{F}$ and $y \text{LiCoPO}_4$ compositions.

Ni and Co amount are decreased towards down direction of triangle; meanwhile the Iron is increased. High Fe value is found at sample 7 and its content decreases at the opposite endpoints of the triangle.

Table 2. 10 different composition points according to using the lever rule, stoichiometric weights and mole-fractions of the triangle diagram.

Composition	
Sample	
1	$\text{LiNi}_{0.333}\text{Co}_{0.333}\text{Fe}_{0.333} \text{PO}_4$
2	$\text{Li}_{1.167}\text{Ni}_{0.278}\text{Co}_{0.278}\text{Fe}_{0.444} \text{PO}_4$
3	$\text{LiNi}_{0.278} \text{Co}_{0.278} \text{Fe}_{0.278}\text{Co}_{0.167} \text{PO}_4$
4	$\text{Li}_{1.333}\text{Ni}_{0.222}\text{Co}_{0.222}\text{Fe}_{0.555} \text{PO}_4$
5	$\text{Li}_{1.167} \text{Ni}_{0.222} \text{Co}_{0.389} \text{Fe}_{0.388} \text{PO}_4$
6	$\text{LiNi}_{0.222} \text{Co}_{0.555} \text{Fe}_{0.222}\text{PO}_4$
7	$\text{Li}_{1.5} \text{Ni}_{0.167} \text{Co}_{0.167} \text{Fe}_{0.667} \text{PO}_4$

Table 3. Summary capacity and cycle-ability for 10 samples, of the system [(1-x-y) LiFe_{0.333}Ni_{0.333}Co_{0.333}] PO₄, x Li₂FePO₄F and yLiCoPO₄ compositions.

Sample	Blend	Li ₂ FePO ₄ F	LiCoPO ₄
1	Pure	0	0
2	Binary	0.167	0
3	Binary	0	0.167
4	Binary	0.333	0
5	Ternary	0.167	0.167
6	Binary	0	0.333
7	Binary	0.500	0
Sample	LiNi _{0.333} Co _{0.333} Fe _{0.333} PO ₄	First discharge Capacity	Cycle-ability
1	1	132.5	46
2	0.833	141.4	45
3	0.833	110.3	55
4	0.667	100.5	50
5	0.667	126.4	60
6	0.667	111.5	60
7	0.500	112.6	80

High Cobalt value is found in sample 1 and its percentage is found in a wide region in the triangle. It is predicted which capacities and cycle-ability of the compositions are directly related to the amount of Fe, Co and Ni. It is notable, specific capacity is determined as the number of energies which can be a reserve in volume or mass (Ah), while the rate capability (which are related to their design and varies considerably between different manufactures), can be determined as the rate at which the cell is being charged. Therefore the C-rate is the capacity of the battery divided by the hourly charging rate. The discharge capacity curves of this work have been compared with 18650-type “C/LiCoO₂ Sony battery” result which is modified by Ehrlich [69]. Since LiCoO₂ cathode has an initial discharge capacity around 145mAh/g [39], therefore any materials of these compositions with initial capacities more than this amount (of course with a suitable cycle-ability) might be considered. The samples were tested via a cycler (Arbin BT 2000 battery testing system), between 2.4V and 3.8V with low C-rate of C/10. The initial results indicate of a wide range and irregular of cycle-ability and capacities. The initial discharge capacities varied from 100.5 to 141.4 “mAhg⁻¹”. Both capacity and cycle-ability increase from LiFe_{0.333}Ni_{0.333}Co_{0.333}PO₄ towards the binary compositions.

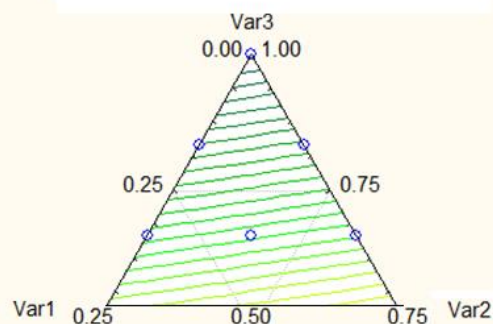


Figure 3. Ternary of capacity versus Var₁, Var₂ and Var₃ for 28 samples of {[(1-x-y) LiFe_{0.333}Ni_{0.333}Co_{0.333}] PO₄}, xLi₂FePO₄F and yLiCoPO₄ composites.

Although sample 2 shows high capacity of “141.4” mAhg⁻¹, it contains of a low cycle-ability compare to sample 5. The samples 1, 2 and 5 exhibits suitable capacities but only sample 5 is acceptable due to high cycle-ability. Although these kinds of data

are not sufficient for determining a suitable cathode material in viewpoint of capacity and cycle-ability amount, the statistical analysis can be useful for finding the region of the best item from the data of the 7 compositions. Therefore a few testing with both capacity and cycle-ability relation in viewpoint of the triangle regions is needed (Figs. 3, 4). In this work the STATISTICA software has been used for analyzing the data which Var₁, Var₂, Var₃, are Li₂FePO₄, LiCoPO₄ and LiFe_{0.333}Ni_{0.333}Co_{0.333}] PO₄ respectively while the Var₄ alternately, are the capacity and cycle-ability.

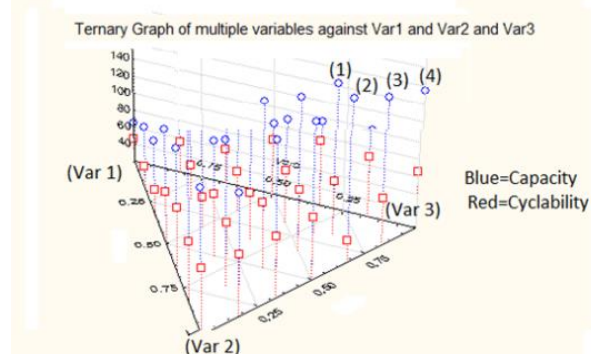


Figure 4. {[(1-x-y) LiFe_{0.333}Ni_{0.333}Co_{0.333}] PO₄}, xLi₂FePO₄F and yLiCoPO₄ composites with high precisionist of capacity and cycle-ability Var₁, Var₂ and Var₃.

Recently a few works have been investigated for increasing the efficiency of cathode materials in LIBs [70-85]. By this work various compositions are used for exploring the novel cathode materials with two-dimensional layered structure through the ternary composition’s diagram among Iso-structural materials. Through an analyzing among these compositions, two samples were chosen and subsequently synthesized, characterized and tested consequently with high precisionist. Via initial discharge capacity and some extra results number 5 as Li_{1.167} Ni_{0.222} Co_{0.389} Fe_{0.388} PO₄ is indicated as the suitable cathode material among those structures. Obviously, the used weight of cobalt in these samples is lower compared with LiCoO₂ that is an advantage in viewpoint of cost and toxic in this study. The repeat of samples was made into T-Cells and subjected to electrochemical testing using the original conditions and the cycling was accomplished between 2.4 - 3.8V with constant C-rate of C/10 at room temperature (Fig. 5).

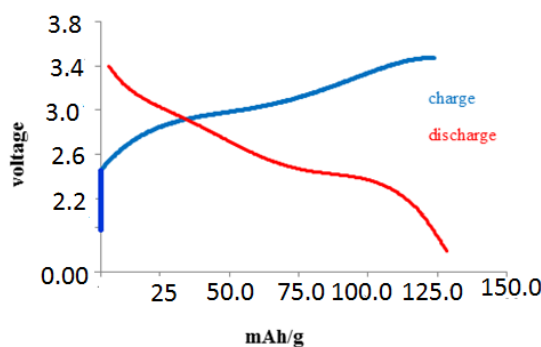


Figure 5. Charge and discharge capacity of Li_{1.167} Ni_{0.222} Co_{0.389} Fe_{0.388} PO₄.

The repeat sample exhibits better charge and discharge capacities and this improvement in the capacities is attributed to the synthesis conditions.

4. CONCLUSIONS

{[(1-x-y) LiFe_{0.333}Ni_{0.333}Co_{0.333}] PO₄}, xLi₂FePO₄F and yLiCoPO₄ composite system of cathodes with submicron particles have been successfully synthesized by a sol-gel method. The structural and electrochemical properties have been systemically investigated to examine the effects of charge/discharge capacities and also capacity retention. The results show that the prepared “Li_{1.167} Ni_{0.222} Co_{0.389} Fe_{0.388} PO₄” type layered structure regardless of the nickel content and Fe, improve the capacity retention

5. REFERENCES

- Cheng, F.; Liang, J.; Tao, Z.; Chen, J. Functional materials for rechargeable batteries. *Advanced Materials* **2011**, *23*, 1695-1715, <https://doi.org/10.1002/adma.201003587>.
- Whittingham, M.S.; Materials challenges facing electrical energy storage. *MRS Bulletin* **2008**, *33*, 411-419, <https://doi.org/10.1557/mrs2008.82>.
- She-huang, Wu. Su, H. S.; Electrochemical characteristics of partially cobalt-substituted LiMn_{2-y}Co_yO₄ spinels synthesized by Pechini process, *Materials Chemistry and Physics* **2002**, *78*, 189-195
- Tarascon, J. M.; Armand, M. Issues and challenges facing rechargeable lithium batteries. *Nature* **2001**, *414*, 359-367, <https://doi.org/10.1038/35104644>.
- Nagaura, T.T.K. Lithium ion rechargeable battery, *Progress in Batteries & Solar Cells*. **1990**, *9*, 209.
- Scrosati, B.; Garche, J. Lithium batteries: Status, prospects and future. *Journal of Power Sources* **2010**, *195*, 2419-2430, <https://doi.org/10.1016/j.jpowsour.2009.11.048>.
- Whittingham, M.S. Lithium Batteries and Cathode Materials. *Chemical Reviews* **2004**, *104*, 4271-4302, <https://doi.org/10.1021/cr020731c>.
- Bruce, P.G.; Scrosati, B.; Tarascon, J.M. Nanomaterials for Rechargeable Lithium Batteries. *Angewandte Chemie International Edition* **2008**, *47*, 2930-2946, <https://doi.org/10.1002/anie.200702505>.
- Goodenough, J.B.; Kim, Y. Challenges for Rechargeable Li Batteries. *Chemistry of Materials* **2009**, *22*, 587-603, <https://doi.org/10.1021/cm901452z>.
- Kaskhedikar, N.A.; Maier, J. Lithium storage in carbon nanostructures. *Advanced Materials* **2009**, *21*, 2664-2680, <https://doi.org/10.1002/adma.200901079>.
- Cabana, J.; Monconduit, L.; Larcher, D.; Palacin, M.R. Beyond intercalation-based Li-ion batteries: The state of the art and challenges of electrode materials reacting through conversion reactions. *Advanced Materials*, **2010**, *22*, 170-192, <https://doi.org/10.1002/adma.201000717>.
- Poizot, P.; Laruelle, S.; Grugeon, S.; Dupont, L.; Tarascon, J.M. Nano-sized transition-metaloxides as negative-electrode materials for lithium-ion batteries. *Nature* **2000**, *407*, 496-499, <https://doi.org/10.1038/35035045>.
- Park, J. C.; Kim, J.;Kwon, H.; Song, H. Gram-Scale Synthesis of Cu₂O Nanocubes and Subsequent Oxidation to CuO Hollow Nanostructures for Lithium-Ion Battery Anode Materials. *Advanced Materials* **2009**, *21*, 803, <https://doi.org/10.1002/adma.200800596>.
- Ban, C.M., Wu, Z.C.; Gillaspie, D.T.; Chen, L.; Yan, Y.F.; Blackburn, J.L.; Dillon, A.C. *Advanced Materials* **2010**, *22*, 145, <https://doi.org/10.1002/adma.200904285>.
- Doh, C.H.; Kalaiselvi, N.; Park, C.W.; Jin, B.S.; Moon, S.I.; Yun, M.S. Synthesis and electrochemical characterization of novel high capacity Si_{3-x}FexN₄ anode for rechargeable lithium batteries. *Electrochemistry Communications* **2004**, *6*, 965-968, <https://doi.org/10.1016/j.elecom.2004.07.011>.
- Cabana, J.; Stoeva, Z.; Titman, J.J.; Gregory, D.H.; Palacin, M.R. Towards new negative electrode materials for Li-ion batteries: Electrochemical properties of Li-Ni-N. *Chemistry of Materials* **2008**, *20*, <https://doi.org/10.1021/cm7034486>.
- Morgan, D.; Van der Ven, A.; Ceder, G. Li conductivity in Li_xMPO₄ (M = Mn, Fe, Co, Ni) olivine materials. *Electrochemical and Solid State Letters* **2004**, *7*, 30-32, <https://doi.org/10.1149/1.1633511>.
- Muraliganth, T.; Murugan, A.V.;Manthiram, A. Nano scale networking of LiFePO₄ nano rods synthesized by a microwave-solvo thermal route with carbon nanotubes for lithium ion batteries. *Journal of Materials Chemistry* **2008**, *18*, 5661-5668, <http://dx.doi.org/10.1039/b812165f>.
- Yamada, A.; Chung, S.C.; Hinokuma, K. Optimized LiFePO₄ for lithium battery cathodes. *Journal of the Electrochemical Society* **2001**, *148*, 224-229, <https://doi.org/10.1149/1.1348257>.
- Wang, Y.G.; Wang, Y.R.; Hosono, E.J.; Wang, K X.; Zhou, H.S. The design of a LiFePO₄/carbon nano-composite with a core-shell structure and its synthesis by an in situ polymerization restriction method. *Angewandte Chemie-International Edition* **2008**, *47*, 7461-7465, <https://doi.org/10.1002/anie.200802539>.
- Zhou, Y.; Wang, J.; Hu, Y.; O'Hayre, R.; Shao, Z. A porous LiFePO₄ and carbon nanotube composite. *Chemical Communications* **2010**, *46*, 7151-7153, <https://doi.org/10.1039/C0CC01721C>.
- Liu, J.; Conry, T.E.; Song, X.; Doeff, M.M.; Richardson, T.J. Nano-porous spherical LiFePO₄ for high performance cathodes. *Energy & Environmental Science*, **2011**, *4*, 885-888, <https://doi.org/10.1039/c0ee00662a>.
- Saravanan, K.; Balaya, P.; Reddy, M.V.; Chowdari, B.V.R.; Vittal, J.J. Morphology controlled synthesis of LiFePO₄/C nano plates for Li-ion batteries. *Energy & Environmental Science*, **2010**, *3*, 457-464, <https://doi.org/10.1039/B923576K>.
- Srinivasan, V.; Newman, J. Discharge model for the lithium iron-phosphate electrode. *Journal of the Electrochemical Society* **2004**, *151*, 1517-1529, <https://doi.org/10.1149/1.1785012>.
- Akimoto, J.; Gotoh, Y.; Oosawa, Y. Synthesis and Structure Refinement of LiCoO₂ Single Crystals. *Journal of Solid State Chemistry* **1998**, *141*, 298-302.
- Madhu, C.; Garrett, J.; Manivannan, V. Synthesis and characterization of oxide cathode materials of the system (1-y)LiNiO_xLiMnO_yLiC_oO. *Ionics* **2010**, *16*, 591-602.
- Sun, Y. The preparation and electrochemical performance of solid solutions LiCoO₂-Li₂MnO₃ as cathode materials for lithium ion batteries. *Journal of Power Sources* **2006**, *159*, 1353-1359, <https://doi.org/10.1016/j.jpowsour.2005.12.037>.
- Jiang, J. Structure, Electrochemical Properties, and Thermal Stability Studies of Cathode Materials in the xLi [Mn 1/2] NiO_y LiCoO_zLi [Li1/3] Mn[2/3] O₂ Pseudoternary System (x + y + z = 1). *Journal of The Electrochemical Society* **2005**, *152*, 1879-1889.

29. Zhong, Q. Synthesis and Electrochemistry of LiNiMn- xO2 *Journal of the Electro-chemical Society* **1997**, *144*, 205-213.
30. Zhong, S.W.; Zhao, Y.J.; Li, Y.; Li, P.Z.; Mei, J.; Liu, Q.G. Characteristics and electrochemical performance of cathode material Co coated LiNiO2 for Li-ion batteries. *Transactions of Nonferrous Metals Society of China* **2006**, *16*, 137-141, [https://doi.org/10.1016/S1003-6326\(06\)60024-1](https://doi.org/10.1016/S1003-6326(06)60024-1).
31. Amatucci, G.; Pasquier, A.D.; Blyr, A.; Zheng, T.; Tarascon, J.M. The elevated temperature performance of the LiMn2O4/C system: failure and solutions. *Electrochimica Acta* **1999**, *45*, 255-271, [https://doi.org/10.1016/S0013-4686\(99\)00209-1](https://doi.org/10.1016/S0013-4686(99)00209-1).
32. Liu, L.; Wang, Z.; Li, H.; Chen, L.; Huang, X. Al2O3-coated LiCoO2 as cathode material for lithium ion batteries. *Solid State Ionics* **2002**, *152*, 341.
33. Mikhaylik, Y.V.; Akridge, J.R. Low Temperature Performance of Li/S Batteries, *J. Electrochem. Soc.* **2003**, *150*, 306.
34. Colfen, H.; Mann, S. Higher-order organization by mesoscale self-assembly and transformation of hybrid nanostructures. *Angewandte Chemie-International Edition* **2003**, *42*, 2350-2365, <https://doi.org/10.1002/anie.200200562>.
35. Colfen, H.; Antonietti, M. Mesocrystals: Inorganic superstructures made by highly parallel crystallization and controlled alignment. *Angewandte Chemie-International Edition* **2005**, *44*, 5576-5591, <https://doi.org/10.1002/anie.200500496>.
36. Yu, S.H.; Colfen, H.; Tauer, K.; Antonietti M. Tectonic arrangement of BaCO3 nanocrystals into helices induced by a racemic block copolymer. *Nature Materials* **2005**, *4*, 51-55, <https://doi.org/10.1038/nmat1268>.
37. Song, R. Q.; Colfen, H. Mesocrystals-ordered nanoparticle superstructures. *Advanced Materials* **2010**, *22*, 1301-1330, <https://doi.org/10.1002/adma.200901365>.
38. Colfen, H.; Antonietti, M. *Mesocrystals and nonclassical crystallization*. 2008, John Wiley & Sons, Ltd.
39. Kanamura, K.; Koizumi, S.H.; Dokko, K.R. Hydrothermal synthesis of LiFePO4 as a cathode material for lithium batteries. *Journal of Materials Science* **2008**, *43*, 2138-2142, <http://dx.doi.org/10.1007/s10853-007-2011-1>.
40. Mollaamin, F.; Najafpour, J.; Ghadami, S.; Akrami, M.S.; Monajjemi, M. The Electromagnetic Feature of B15N15Hx (x=0,4, 8, 12, 16, and 20) Nano Rings: Quantum Theory of Atoms in Molecules/NMR Approach. *Journal of computational and theoretical nanoscience* **2014**, *11*, 1290-1298.
41. Monajjemi, M.; Ahmadianarog, M. Carbon Nanotube as a Deliver for Sulforaphane in Broccoli Vegetable in Point of Nuclear Magnetic Resonance and Natural Bond Orbital Specifications. *Journal of computational and theoretical nanoscience* **2014**, *11*, 1465-1471.
42. Monajjemi, M.; Mahdavian, L.; Mollaamin, F.; Characterization of nanocrystalline silicon germanium film and nanotube in adsorption gas by monte carlo and langevin dynamic simulation, *Bulletin of the chemical society of Ethiopia* **2008**, *22*, 277-286, <https://doi.org/10.4314/bcse.v22i2.61299>.
43. Monajjemi, M.; Ghiasi, R.; Ketabi, S.; Pasdar, H.; Mollamin, F. A theoretical study of metal-stabilised rare tautomers stability: N4 metalated cytosine (M=Be2+, Mg2+, Ca2+, Sr2+ and Ba2+) in gas phase and different solvents. *Journal of chemical research* **2004**, *1*, 11-18, <https://doi.org/10.3184/030823404323000648>.
44. Monajjemi, M.; Ghiasi, R.; Sadjadi, M.A.S. Metal-stabilized rare tautomers: N4 metalated cytosine (M = Li+, Na+, K+, Rb+ and Cs+), theoretical views. *Applied organometallic chemistry* **2003**, *17*, 635-640, <https://doi.org/10.1002/aoc.469>.
45. Monajjemi, M.; Mahdavian, L.; Mollaamin, F.; Honarparvar, B. Thermodynamic Investigation of EnolKeto Tautomerism for Alcohol Sensors Based on Carbon Nanotubes as Chemical Sensors. *Fullerenes nanotubes and carbon nanostructures* **2010**, *18*, 45-55, <https://doi.org/10.1080/15363830903291564>.
46. Hadad, B.K.; Mollaamin, F.; Monajjemi, M. Biophysical chemistry of macrocycles for drug delivery: a theoretical study. *Russian chemical bulletin* **2011**, *60*, 238-241, <https://doi.org/10.1007/s11172-011-0039-5>.
47. Monajjemi, M.; Honarparvar, B.; Hadad, B.K.; Ilkhani, A.R.; Mollaamin F. Thermo-chemical investigation and NBO analysis of some anxileotic as Nano- drugs. *African journal of pharmacy and pharmacology* **2010**, *4*, 521-529.
48. Monajjemi, M.; Naderi, F.; Mollaamin, F.; Khaleghian, M. Drug Design Outlook by Calculation of Second Virial Coefficient as a Nano Study. *Journal of the mexican chemicalsociety* **2012**, *56*, 207-211.
49. Monajjemi, M.; Mohammadian, N.T.S-NICS an Aromaticity Criterion for Nano Molecules. *J. Comput. Theor. Nanosci* **2015**, *12*, 4895-4914.
50. Monajjemi, M.; Lee, V.S.; Khaleghian, M.; Honarparvar, B.; Mollaamin, F. Theoretical Description of Electromagnetic Nonbonded Interactions of Radical, Cationic, and Anionic NH2BHNBNH2 Inside of the B18N18 Nanoring. *J. Phys. Chem C* **2010**, *114*, 15315, <http://dx.doi.org/10.1021/jp104274z>.
51. Monajjemi, M.; Boggs, J.E.; A New Generation of BnNn Rings as a Supplement to Boron Nitride Tubes and Cages. *J. Phys. Chem. A* **2013**, *117*, 1670-1684, <http://dx.doi.org/10.1021/jp312073q>.
52. Monajjemi, M. Non bonded interaction between BnNn (stator) and BN B (rotor) systems: A quantum rotation in IR region. *Chemical Physics* **2013**, *425*, 29-45, <https://doi.org/10.1016/j.chemphys.2013.07.014>.
53. Monajjemi, M.; Robert, W.J.; Boggs, J.E. NMR contour maps as a new parameter of carboxyl's OH groups in amino acids recognition: A reason of tRNA-amino acid conjugation. *Chemical Physics* **2014**, *433*, 1-11, <https://doi.org/10.1016/j.chemphys.2014.01.017>.
54. Monajjemi, M. Quantum investigation of non-bonded interaction between the B15N15 ring and BH2NBH2 (radical, cation, and anion) systems: a nano molecularmotor. *Struct Chem* **2012**, *23*, 551-580, <http://dx.doi.org/10.1007/s11224-011-9895-8>.
55. Monajjemi, M. Non-covalent attraction of B2N (2, 0) and repulsion of B2N (+) in the BnNn ring: a quantum rotatory due to an external field. *Theor Chem Acc* **2015**, 1668-9, <https://doi.org/10.1007/s00214-015-1668-9>.
56. Monajjemi, M. Metal-doped graphene layers composed with boron nitride-graphene as an insulator: a nano-capacitor. *Journal of Molecular Modeling* **2014**, *20*, 2507, <https://doi.org/10.1007/s00894-014-2507-y>.
57. Ilkhani, A.R.; Monajjemi, M. The pseudo Jahn-Teller effect of puckering in pentatomic unsaturated rings C(4)AE(5), A = N, P, As, E = H, F, Cl. *Computational and theoretical chemistry* **2015**, *1074*, 19-25.
58. Monajjemi M. Graphene/(h-BN)(n)/X-Doped Graphene As Anode Material in Lithium Ion Batteries. *Macedonian Journal of Chemistry and Chemical Engineering* **2017**, *36*, 101-118, <https://doi.org/10.20450/mjce.2017.1134>.
59. Monajjemi, M.; Najafpour, J.; Charge density discrepancy between NBO and QTAIM in single-wall armchair carbon nanotubes. *Fullerenes Nanotubes and Carbon Nanostructures* **2014**, *22*, 575-594, <https://doi.org/10.1080/1536383X.2012.702161>.
60. Monajjemi, M. Cell membrane causes the lipid bilayers to behave as variable capacitors: A resonance with self-induction of helical proteins. *Biophysical Chemistry* **2015**, *207*, 114-127, <https://doi.org/10.1016/j.bpc.2015.10.003>.
61. Mollaamin, F.; Monajjemi, M. DFT outlook of solvent effect on function of nano bioorganic drugs. *Physics and Chemistry of Liquids* **2012**, *50*, 596-604, <https://doi.org/10.1080/00319104.2011.646444>.

62. Monajjemi, M.; Chegini, H.; Mollaamin, F.; Farahani, P. Theoretical Studies of Solvent Effect on Normal Mode Analysis and Thermodynamic Properties of Zigzag (5,0) carbon nanotube. *Fullerens Nanotubes carbon and nanostructures* **2011**, *19*, 469-482, <https://doi.org/10.1080/1536383X.2010.494783>.
63. Monajjemi, M. Study of CD5+ Ions and Deuterated Variants ($\text{CH}_x\text{D}(5-x)^+$): An Artefactual Rotation. *Russian Journal of Physical Chemistry a* **2018**, *92*, 2215-2226.
64. Monajjemi, M.; Baei, M.T.; Mollaamin, F. Quantum mechanics study of hydrogen chemisorptions on nanocluster vanadium surface. *Russian journal of inorganic chemistry* **2008**, *53*, 1430-1437, <https://doi.org/10.1134/S0036023608090143>.
65. Monajjemi, M. Liquid-phase exfoliation (LPE) of graphite towards graphene: An ab initio study. *Journal of Molecular Liquids* **2017**, *230*, 461-472, <https://doi.org/10.1016/j.molliq.2017.01.044>.
66. Monajjemi, M.; Mahdavian, L.; Mollaamin, F. Interaction of Na, Mg, Al, Si with carbon nanotube (CNT): NMR and IR study. *Russian Journal of Inorganic Chemistry* **2009**, *54*, 1465-1473, <http://dx.doi.org/10.1134/S0036023609090216>.
67. Monajjemi, M.; Ahmadianarog, M. Carbon Nanotube as a Deliver for Sulforaphane in Broccoli Vegetable in Point of Nuclear Magnetic Resonance and Natural Bond Orbital Specifications. *Journal of computational and theoretical nanoscience* **2014**, *11*, 1465-1471, <https://doi.org/10.1166/jctn.2014.3519>.
68. Lee, V.S.; Nimmanpipug, P.; Mollaamin, F.; Kungwan, N.; Thanasanvorakun, S.; Monajjemi, M. Investigation of single wall carbon nanotubes electrical properties and mode analysis: Dielectric effects. *Russian journal of physical chemistry A* **2009**, *83*, 2288-2296, <https://doi.org/10.1134/S0036024409130184>.
69. Ehrlich, G.M.; Linden, D. *Handbook of Lithium-ion batteries*, McGraw-Hill, New york, 2002, pp. 35.
70. Schipper, F.; Nayak, P.K.; Erickson, E.M.; Amalraj, S.F.; Srur-Lavi, O.; Penki, T.R.; Talianker, M.; Grinblat, J.; Sclar, H.; Breuer, O.; Julien, C.M.; Munichandraiah, N.; Kovacheva, D.; Dixit, M.; Major, D.T.; Markovsky, B.; Aurbach, D. Study of Cathode Materials for Lithium-Ion Batteries: Recent Progress and New Challenges. *Inorganics* **2017**, *5*, 32, <https://doi.org/10.3390/inorganics5020032>.
71. Erickson, E.M.; Schipper, F.; Penki, T.R.; Shin, J.-Y.; Erk, C.; Chesneau, F.F.; Markovsky, B.; Aurbach, D. Review—recent advances and remaining challenges for lithium ion battery cathodes: II. Lithium-rich, $\text{xLi}_2\text{MnO}_3 \cdot (1-x)\text{LiNiO}_2$. *J. Electrochem. Soc.* **2017**, *164*, 6341-6348, <https://doi.org/10.1149/2.0461701jes>.
72. Wang, Z.; Sun, L.; Yang, W.; Yang, J.; Sun, K.; Chen, D.; Liu, K. Unveiling the Synergic Roles of Mg/Zr Co-Doping on Rate Capability and Cycling Stability of $\text{Li}_4\text{Ti}_5\text{O}_{12}$. *J. Electrochem. Soc.* **2019**, *166*, 658-666, <https://doi.org/10.1149/2.0791904jes>.
73. Koo, B.; Yi, J.; Dongcheul Lee, Shin, C.B.; Park, S. Modeling the Effect of Fast Charge Scenario on the Cycle Life of a Lithium-Ion Battery. *J. Electrochem. Soc.* **2018**, *165*, 3674-3683, <https://doi.org/10.1149/2.0281816jes>.
74. Sarkar, A.; Shrotriya, P.; Chandra, A. Parametric Analysis of Electrode Materials on Thermal Performance of Lithium-Ion Battery: A Material Selection Approach. *J. Electrochem. Soc.* **2018**, *165*, 1587-1594, <https://doi.org/10.1149/2.0061809jes>.
75. Sun, D.; Miao, X.; Yang, J.; Li, H.; Zhou, X.; Lei, Z. MoS_2 Nanosheets Vertically Aligned on Hierarchically Porous Graphitic Carbon for High-Performance Lithium Storage. *J. Electrochem. Soc.* **2018**, *165*, 2859-2865, <https://doi.org/10.1149/2.0011813jes>.
76. Yu, L.; Jun, Y.; Lin, Y.S. Ceramic coated polypropylene separators for lithium-ion batteries with improved safety: effects of high melting point organic binder. *RSC Advances* **2016**, *6*, 40002, <http://dx.doi.org/10.1039/C6RA04522G>.
77. Petibon, R.; Xia, J.; Ma, L.; Bauer, M.K.G.; Nelson, K.J.; Dahn, J.R. Electrolyte System for High Voltage Li-Ion Cells. *J. Electrochem. Soc.* **2016**, *163*, 2571, <https://doi.org/10.1149/2.0321613jes>.
78. Blomgren, G.E. The Development and Future of Lithium Ion Batteries. *Journal of The Electrochemical Society* **2017**, *164*, 5019-5025, <http://dx.doi.org/10.1149/2.0251701jes>.
79. Duhnen, S.; Nolle, R.; Wrogemann, J.; Winter, M.; Placke, T. Reversible Anion Storage in a Metal-Organic Framework for Dual-Ion Battery Systems. *Journal of The Electrochemical Society* **2019**, *166*, 5474-5482, <https://doi.org/10.1149/2.0681903jes>.
80. Galushkin, N.E.; Yazvinskaya, N.N.; Galushkin, D.N. Mechanism of Gases Generation during Lithium-Ion Batteries Cycling. *Journal of The Electrochemical Society* **2019**, *166*, 897-908, <https://doi.org/10.1149/2.0041906jes>.
81. Tchitchekova, D.S.; Frontera, C.; Ponrouch, A.; Krich, C.; Bardé, F.; Palacín, M.R. Electrochemical calcium extraction from $1\text{D-Ca}_3\text{Co}_2\text{O}_6$. *Dalton Trans.* **2018**, *47*, 11298-11302.
82. Tchitchekova, D.S.; Monti, D.; Johansson, P.; Bardé, F.; Randon-Vitanova, A.; Palacín, M.R.; Ponrouch, A. On the Reliability of Half-Cell Tests for Monovalent (Li^+ , Na^+) and Divalent (Mg^{2+} , Ca^{2+}) Cation Based Batteries. *J. Electrochem. Soc.* **2017**, *164*, A1384-A1392.
83. Zarrabeitia, M.; Muñoz-Márquez, M.; Nobili, F.; Rojo, T.; Casas-Cabanas, M. Influence of Using Metallic Na on the Interfacial and Transport Properties of Na-Ion Batteries. *Batteries* **2017**, *3*, 16.
84. Schmich, R.; Wagner, R.; Hörpel, G.; Placke, T.; Winter, M. Performance and cost of materials for lithium-based rechargeable automotive batteries. *Nat. Energy* **2018**, *3*, 267-278.
85. Wandt, J.; Lee, J.; Arrigan, D.W.M.; Silvester, D.S. A lithium iron phosphate reference electrode for ionic liquid electrolytes. *Electrochem. Commun.* **2018**, *93*, 148-151.

6. ACKNOWLEDGEMENTS

"This research is funded by Vietnam National University – Ho Chi Minh city (VNU-HCM) under the grand number TX2019-32-01."



© 2019 by the authors. This article is an open access article distributed under the terms and conditions of the Creative Commons Attribution (CC BY) license (<http://creativecommons.org/licenses/by/4.0/>).